

IMECE2007-42831

METAL HYDRIDE HEAT STORAGE TECHNOLOGY FOR DIRECTED ENERGY WEAPON SYSTEMS

¹Chanwoo Park and Xudong Tang
Advanced Cooling Technologies, Inc.,
1046 New Holland Avenue, Lancaster, PA 17601
¹e-mail: chanwoo.park@1-act.com

Kwang J. Kim
Active Materials and Processing Laboratory
Mechanical Engineering, University of Nevada, Reno, NV 89557

Joseph Gottschlich and Quinn Leland
Air Force Research Laboratory, WPAFB, Dayton, OH

ABSTRACT

Directed Energy Weapon (DEW) systems in a pulse operation mode dissipate excessively large, transient waste heat because of their inherent inefficiencies. The heat storage system can store such a pulsed heat load not relying on oversized systems and dissipate the stored heat over time after the pulse operation. A compressor-driven metal hydride heat storage system was developed for efficient, compact heat storage and dissipation of the transient heat from the DEW systems. The greater volumetric heat storage capacity of metal hydride material was realized into more compact design than conventional Phase Change Material (PCM) systems. Other exclusive advantages of the metal hydride system were fast thermal response time and active heat pumping capability required for precision temperature control and on-demand cooling. This paper presented the operating principle and heat storage performance results of the compressor-driven metal hydride heat storage system through system modeling and prototype testing. The modeling and test results showed that the metal hydride system can store the average heat of 4.4kW during the heat storage period of 250 seconds and release the stored heat during the subsequent regeneration period of 900 seconds.

KEYWORDS

Heat storage, thermal, cooling, metal hydride, phase change material, directed energy weapon, solid state laser, compressor

NOMENCLATURE

A_p	Reaction prefactor [kmole H ₂ /kmole hyd-s]	E_a	Activation energy [J/kmole H ₂]
H/M	Hydrogen concentration in hydride	h	Heat transfer coefficient [W/m ² -K]
\bar{m}	Hydrogen mass flow rate [kg/s]	N_0	Hydride particle molar mass [kmole hyd/particle hyd]
p	Pressure [atm]	Q	Heat transfer rate [W]
R	Universal gas constant [8.314 kJ/kgmole-K]	T	Temperature [K]
\dot{S}	Heat generation rate in hydriding/dehydriding [W/m ³]	t	Time [sec]
V	Volume [m ³]	x	Non-stoichiometric constant

Greek

α, β	Metal hydride phase	ΔH_f	Heat of formation [kJ/H ₂ -kgmole]
ΔS_f	Standard entropy of formation [kJ/H ₂ -kgmole-K]	ε	Metal hydride porosity
\mathfrak{R}	Hydride particle density [particle hyd/m ³]		
Subscripts			
<i>A</i>	Metal hydride reactor	<i>B</i>	Hydrogen container
<i>C</i>	Hydrogen compressor	<i>s</i>	Hydrogen solid phase in hydride
<i>f</i>	Hydrogen fluid phase	<i>w</i>	Water

INTRODUCTION

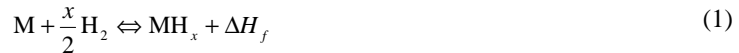
Recent advances of high power solid state lasers promises necessary laser power levels required for the Directed Energy Weapons (DEW) systems. However, inefficiencies of the laser components still generate too much waste heat to be managed by conventional liquid cooling systems, especially in an airborne platform where compactness, light-weight and energy-efficiency are the primary requirements. The DEW systems typically operate in a pulse mode generating very high peak heat that exceeds the capacities of conventional cooling systems. A heat storage system can be a solution to manage such highly transient heat loads and improve system performance without relying on oversized cooling systems.

Conventional heat storage systems have used Phase Change Materials (PCMs) such as paraffin wax [Mohammed, et al., 2004; Wei, et al., 2005; Vrable and Yerkes, 1998; Shanmugasundaram, et al., 1997]. The PCM systems typically suffer from low thermal conductivities and consequently have to use bulky host structures of high thermal conductivity materials for heat transfer enhancement. In addition, the PCMs' low heat storage density requires excessively large system volumes to meet the DEW heat storage system requirements.

In contrast, the metal hydride systems can provide superior volumetric heat storage capacity as compared to the PCMs. For example, Ca_{0.2}M_{0.8}Ni₅, a commercial hydride, has a heat storage density of 853.3MJ/m³ in raw material condition [Huston and Sandrock, 1980], while paraffin (Calwax 130), a common organic PCM has a heat storage capacity of 177.5MJ/m³ [Al-Hallaj and Selman, 2000]. The greater volumetric heat storage capacity of metal hydride material means more compact design than conventional Phase Change Material (PCM) systems [Park et al., 2005]. Other exclusive advantages of the metal hydride system are fast thermal response time and active heat pumping capability required for precision temperature control and on-demand cooling. The following sections discuss the operating principle and heat storage performance results of the compressor-driven metal hydride heat storage system through system analysis and prototype testing.

PRINCIPLE OF OPERATION

Metal hydrides are the binary combination of hydrogen and a metal or metal alloy. Metal hydrides have been used in many industrial applications such as battery electrode material, hydrogen storage medium and heat pump system [Park et al., 2005; Kang et al., 1996; Fateev et al., 1996; Lloyd et al., 1998; Kim et al., 1998a, 1998b; Houston and Sanrock, 1980]. The hydriding (exothermic) and dehydriding (endothermic) reactions of a metal hydride can be expressed as:



where M is a metal (or metal alloy), x is a non-stoichiometric constant and ΔH_f is the hydride formation heat. Note that metal hydrides are capable of storing an amount of hydrogen gas (STP) equal to about 1,000 times of their own volume. The hydriding/dehydriding reaction kinetics of the hydrides are very rapid and hydride materials are know to be environmentally clean and safe.

Figures 1(a) and (b) show the Pressure-Hydrogen Concentration-Temperature (p-H/M-T) curves for a common metal hydride, LaNi₅H₆ and the van't Hoff plots for commercial hydrides respectively [Houston and Sandrock, 1980]. The p-H/M-T curves and van't Hoff plots contain the key thermodynamic information required for designing any metal hydride systems.

Figure 1(b) shows the van't Hoff plots of commercial metal hydrides. Each line describes the equilibrium behavior of a metal hydride at the *mid-point* of the *desorption* isotherm plateau and the equilibrium behavior is expressed as follows:

$$\ln p_{H_2} (atm) = \frac{\Delta H_f}{RT} - \frac{\Delta S_f}{R} \quad (2)$$

where, R is the universal gas constant [8.314 kJ/kgmole-K], T is the temperature [K], ΔH_f is the heat of formation [kJ/H₂-kgmole] and ΔS_f is the standard entropy of formation [kJ/H₂-kgmole-K]. In the figure, within the temperature range of interest (10~50°C) for the solid state laser cooling, there are various hydrides available from Ca_{0.2}M_{0.8}Ni₅ at higher pressures to Fe_{0.8}Ni_{0.2}Ti at lower pressures.

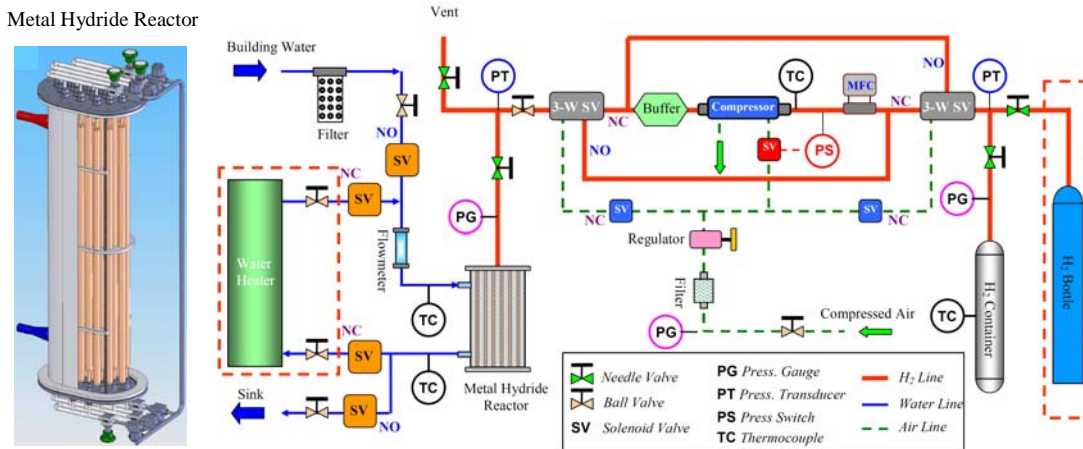


Figure 3 Schematic of compressor-driven metal hydride heat storage system.

The metal hydride reactor adopted a shell-and-tube heat exchanger design where the coolant flows around metal hydride reactor tube bundles. The coolant flow was guided by partitioning baffles to create a serpentine, cross flow inside the heat exchanger. Each hydride reactor tube in the heat exchanger was properly spaced to maximize the convective heat transfer while creating a small flow resistance. The hydride reactor tube was made of a brass tube of 26" long and 0.5" ID. Total 42 hydride reactor tubes were used for a hydride reactor shell. For the hydrogen flow passage and volume change in the hydride reactor tubes, porous screen tube of stainless steel were inserted in the center of each reactor tube.

Table 1 Baseline design specifications of metal hydride heat storage system.

Metal Hydride	$\text{Ca}_{0.6}\text{Mm}_{0.4}\text{Ni}_5$
Laser Heat Source Temperature ($^{\circ}\text{C}$)	30
Heat Sink Temperature ($^{\circ}\text{C}$)	25
Heat Storage Period (sec)	250
Regeneration Period (sec)	500
Hydrogen Container Volume (liter)	50
Hydrogen Charge (mol)	70
Metal Hydride Weight (kg)	10

The baseline design specifications of the metal hydride heat storage system are summarized in Table 1. As shown in Figure 3, the water heater system was used to simulate a laser heat source at constant temperatures during the heat storage. The building water was used as heat sink to cool down the system during the system regeneration. During the heat storage, the water heater system as heat source transports and stores the heat into the metal hydride reactor. The hydrogen generated during dehydriding (endothermic) reaction from the hydride reactor is released and compressed into a hydrogen container by a hydrogen compressor. During the subsequent regeneration, the hydrogen is recovered from the hydrogen container to the hydride reactor. The heat generated by hydriding (exothermic) reaction is gradually removed by the building water as heat sink. Two 3-way pneumatic solenoid valves were used to regulate the hydrogen flow. The water loop was also controlled by a set of electric solenoid valves. Mechanical compression was used to reduce the volume of the hydrogen container, which makes possible to achieve a compact design and maximize the heat storage performance.

METAL HYDRIDE HEAT STORAGE SYSTEM THERMAL MODEL

In order to predict the heat storage performance of the metal hydride system, a lumped thermal model was developed using thermal network modeling. The lumped model had the temperature nodes for a metal hydride reactor, heating/cooling fluid, a compressor and a hydrogen container. The lumped model included dehydriding/hydriding reaction, convective heat transfer and isothermal hydrogen compression.

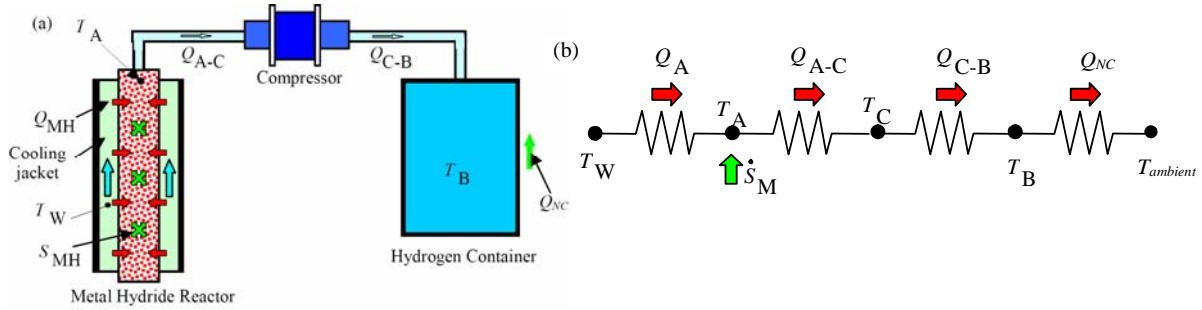


Figure 4 Thermal network model of the compressor-driven metal hydride heat storage system.

Figure 4 shows the thermal network model with the heat flux vectors between temperature nodes. The governing equations for this lumped model are discussed below.

Mass conservation equations of the metal hydride system consisting of metal hydride reactor and hydrogen container are expressed as below.

$$\left((\mathcal{E}V) \frac{d\rho_{H_2}}{dt} \right)_A = (\dot{m}_{H_2} V)_A - \bar{m}_{A-B} \quad (3)$$

$$\left(V \frac{d\rho_{H_2}}{dt} \right)_B = \bar{m}_{A-B} \quad (4)$$

where, \mathcal{E} is the porosity of the metal hydride bed, V is the total volumes of the metal hydride reactor. \dot{m}_{H_2} is the volumetric hydrogen generation rate in the metal hydride bed and is expressed as below.

$$(\dot{m}_{H_2})_A = \left(\frac{1}{2} N_0 \frac{\partial x}{\partial t} M_{H_2} \mathfrak{R} \right)_A \quad (5)$$

where, N_0 is the particle molar mass [kmole hyd/particle hyd], \mathfrak{R} is the particle density [particle hyd/m³], and M_{H_2} is the molecular mass of hydrogen gas [kg/kmole H₂]. x is the hydrogen-to-metal-atomic ratio and $\partial x / \partial t$ is the local reaction rate in the metal hydride bed.

\bar{m}_{A-B} is the hydrogen mass flowrate between the metal hydride reactor (A) and hydrogen container (B). The hydrogen mass flowrate through the compressor varies by a function of drive air pressure and flowrate as well as inlet/outlet hydrogen pressures. The predicted compressor performance curve as shown in Figure 5 was used for the lumped model. Considering the hydrogen compatibility, compression ratio, flowrate, size, weight and cost, a Haskel hydrogen compressor (Model: AGD-7) was chosen for the metal hydride system. The compressor is a pneumatic, double-acting, single-stage oil-free booster. An intercooling during the compression was provided by the drive air flowing through the cooling jacket around the hydrogen barrel of the compressor. The compressor is capable of boosting the hydrogen gas from an inlet pressure of as low as 25 psig to outlet pressure of 400 psig using the drive air of 90 psig and 72 scfm.

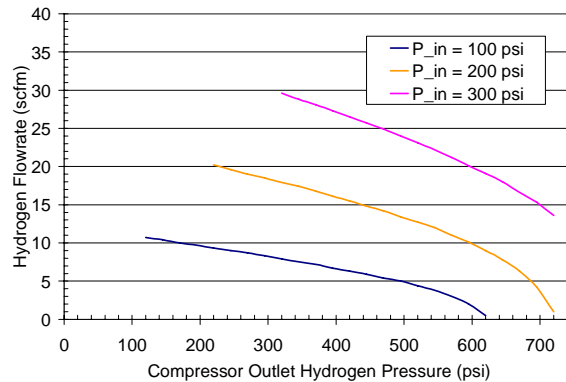


Figure 5 Compressor (manufacturer: Haskel, model: AGD-7) performance prediction.

The energy conservation equations for the metal hydride system are expressed as below.

$$\frac{d}{dt} \left\{ [(1-\varepsilon)(\rho c_v)_s V + \varepsilon(\rho c_v)_f V] \cdot T \right\}_A = \dot{S}_A + Q_A - Q_{A-C} \quad (6)$$

$$\frac{d}{dt} [\rho c_v V]_B = Q_{NC} + Q_{C-B} \quad (7)$$

where, Q_A is the heat transferred into the metal hydride reactor as below. T_w is the heat exchanger inlet coolant temperature. The heat exchanger outlet temperature was assumed to be equal to the reactor temperature T_A . m_w is the water mass flowrate through the reactor.

$$Q_A = m_w C_w (T_w - T_A) \quad (8)$$

Q_{A-C} is the enthalpy flow between the reactor and compressor and Q_{C-B} is the enthalpy flow between the compressor and hydrogen container. It was assumed that the compressor has a perfect intercooling and the hydrogen coming out of the compressor has the same temperature as ambient. Therefore, the enthalpy flows by the hydrogen flow are expressed as below.

$$Q_{A-C} = \bar{m}_{A-B} c_p T^* \begin{cases} T^* = T_A & \bar{m}_{A-B} > 0 \\ T^* = T_{Ambient} & \bar{m}_{A-B} < 0 \end{cases} \quad (9)$$

$$Q_{C-B} = \bar{m}_{A-B} c_p T^* \begin{cases} T^* = T_{Ambient} & \bar{m}_{A-B} > 0 \\ T^* = T_B & \bar{m}_{A-B} < 0 \end{cases} \quad (10)$$

\dot{S}_A is the volumetric heat generation rate during hydriding/dehydriding reactions and is expressed as below.

$$\frac{\dot{S}_A}{V_A} = \left(\frac{1}{2} N_0 \frac{\partial x}{\partial t} \Delta H_f \mathfrak{R} \right)_A \quad (11)$$

where, ΔH_f is the formation energy of hydriding/dehydriding reactions. Arrhenius-type formulation of local reaction rate is expressed as below.

$$\left(\frac{\partial x}{\partial t} \right)_A = \left[A_{rp} \cdot e^{-\frac{E_a}{RT}} \ln \left(\frac{p_{H_2}}{p_{eq}} \right) \right]_A \quad (12)$$

where, E_a is the activation energy [J/kmole H₂] and A_{rp} is the reaction prefactor [kmole H₂/kmole hyd-s].

The Van't Hoff equation for the equilibrium pressure p_{eq} was modeled for the plateau regions using a linear correlation and is expressed as below.

$$\left[\ln(p_{MH,eq}) \right]_A = \left[\frac{\Delta H}{RT} - \frac{\Delta S_f}{R} + \Delta \ln p_x \left(\frac{x - x_{\alpha,max}}{x_{\beta,min} - x_{\alpha,max}} \right) + \begin{cases} \ln \left(\frac{p_a}{p_d} \right) & \text{absorption} \\ 0 & \text{desorption} \end{cases} \right]_A \quad (13)$$

where, ΔS_f is the formation entropy of metal hydride. $x_{\alpha,max}$ is the maximum hydrogen concentration of the hydrogen-depleted metal hydride and $x_{\beta,min}$ is the minimum hydrogen concentration of the hydrogen-saturated metal hydride. $\ln(p_a/p_d)$ represents the hysteresis effect between the hydriding/dehydriding processes.

RESULTS AND DISCUSSION

Before testing, the metal hydride material was activated by removing the pre-formed oxidation layer on the hydride particles and any other impurities. The activation process consisted of several cycles of vacuum baking and hydriding/dehydriding.

To maximize the heat storage performance of the metal hydride system within a given temperature range, the equilibrium pressure of the hydride material has to be carefully chosen. If the equilibrium pressure is too low, the heat storage performance would be degraded because of the slow hydrogen gas flow due to the low pressure differential between the metal hydride reactor and hydrogen container. If the equilibrium pressure is too high, it would be difficult to recover the hydrogen from the hydrogen container by compression. Based on the considerations and some preliminary test results, Ca_{0.6}Mm_{0.4}Ni₅ was selected for the prototype metal hydride heat storage system. The pressure-hydrogen concentration-temperature (p-H/M-T) curves of the metal hydride used for the lumped modeling were calibrated against the measurement results as shown in Figure 6.

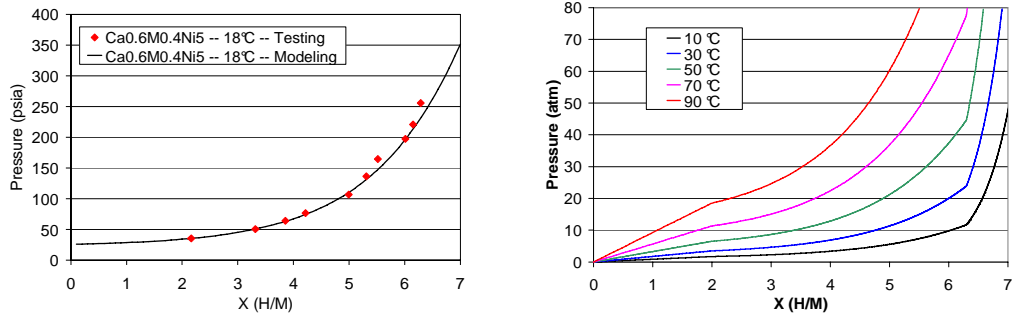


Figure 6 Pressure- Hydrogen Concentration-Temperature curves of $\text{Ca}_{0.6}\text{Mm}_{0.4}\text{Ni}_5$.

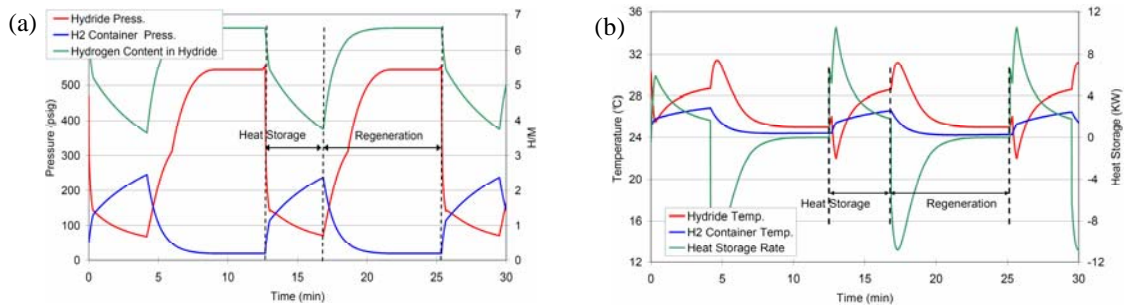


Figure 7 Modeling results of metal hydride heat storage system with 70 mol H_2 charge: (a) temperature and heat transfer and (b) pressure and hydrogen concentration.

The transient behavior of the metal hydride heat storage system was simulated using the lumped thermal model. The variations of pressure, temperature and hydrogen concentration during three consecutive cycles are shown in Figure 7. At the beginning of the heat storage as shown in Figure 7(a), the metal hydride was fully saturated with 550 psi hydrogen while the hydrogen container remains almost empty. The fully-charged metal hydride created a maximum pressure differential between the hydride reactor and hydrogen container, which generated a large hydrogen flowrate and consequently yielded a great heat storage performance. Once the hydride released hydrogen, the temperature of the hydride suddenly dropped due to rapid endothermic reaction. In contrast, the temperature in the hydrogen container rose due to the hydrogen compression. The hydrogen flowrate gradually decreased as the heat storage was close to end, so did the heat storage performance. During the heat storage period, the average heat storage rate of 4.7 kW (or 1.2 MJ for 250 sec) was estimated for 70 mol H_2 charge. It was also showed that during the regeneration, the exothermic reaction driven by compressor created a big temperature differential between the hydride reactor and coolant (heat sink) and accelerated the regeneration process. Note that the compressor was used both during the heat storage and regeneration. Once the system is fully regenerated, the hydrogen line is closed and the system is ready for next duty cycle.

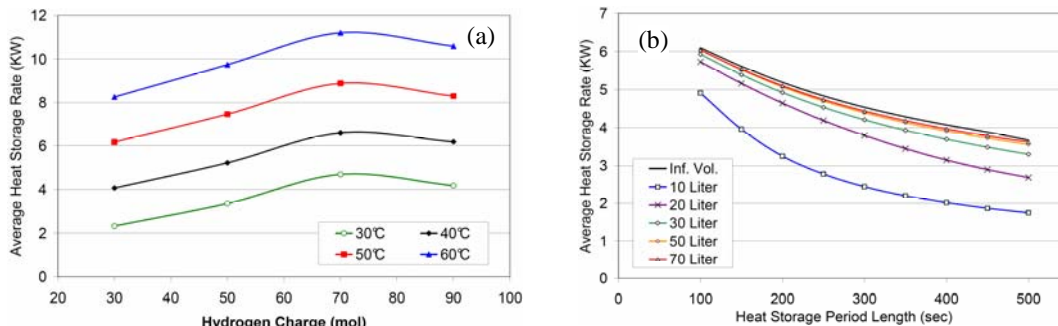


Figure 8 Modeling results of the metal hydride heat storage performance.

Parametric modeling studies were performed using various parameters such as hydrogen container volume, heat storage period, hydrogen charge and heat source temperature. Figure 8(a) shows that there is an optimal value (~70 mole H_2) of the hydrogen charge for maximum heat storage performance. Insufficient hydrogen charge causes inefficient use of the hydride,

while excessive hydrogen charge results in pre-occupied hydrogen container during the heat storage. The higher heat source temperature improves the heat storage performance as shown in Figure 8(a) because of higher hydrogen equilibrium pressure of the metal hydride. Although a small hydrogen container volume would be always preferred, the quick pressure build-up in the small hydrogen container degrades the heat storage performance as shown in Figure 8(b). However, more hydrogen container volume does not always improve the heat storage, because the regeneration process slows down with lower compressor inlet pressure. Therefore, 50-liter hydrogen container volume was selected in our design.

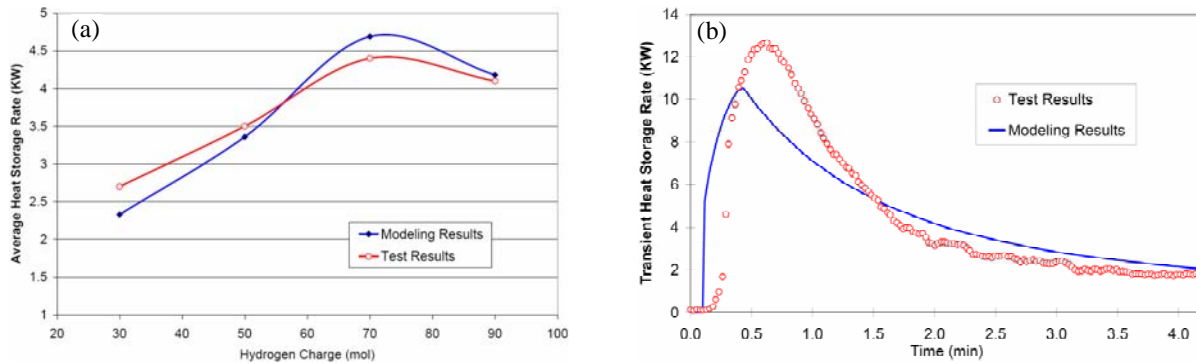


Figure 9 Comparison between test and modeling results of the metal hydride heat storage system: (a) average heat storage rate vs. hydrogen charge and (b) transient heat storage rate for 70 mol H₂ charge.

The prototype metal hydride heat storage system was fabricated and tested for verification. The measurement results were compared against the modeling prediction as shown in Figure 9. It can be seen from Figure 9(a) that the test results had a good agreement with the modeling results on the overall heat storage performance, especially predicting the optimum hydrogen charge. The optimal hydrogen charge for the metal hydride system was around 70 mol H₂. The optimum condition was capable of storing 1.1MJ heat over 250 seconds (i.e., 4.4 kW average heat storage rate) at 30°C heat source temperature. The regeneration time used for the test was 900 seconds. The transient behavior of the heat storage performance during the heat storage period was compared between the measurement and modeling in Figure 9(b). Both of them showed fast heat storage at the early beginning of the heat storage period and slow decline afterwards. The deviation between the modeling prediction and test results, especially in the transient behavior, was attributed to the followings: (1) lump model cannot accurately capture the temperature distribution along the reactor; (2) the hydrogen source/sink terms do not consider the hydride volume change during hydriding/dehydriding, which affects the hydrogen flow in the metal hydride reactor; (3) the compressor performance curve was predicted by a software of the compressor manufacturer for constant pressure boundary conditions.

CONCLUSIONS

The compressor-driven metal hydride heat storage system was developed and the heat storage performance of the system was measured using a prototype hardware. A lumped thermal model was developed to predict the transient heat storage performance of the metal hydride system. The parametric studies were performed to optimize the system design variables and operating conditions. The followings are some of the highlights of this work:

- The average heat storage of 4.4 kW was measured during a heat storage period of 250 seconds.
- High duty cycle (heat storage period of 250 seconds and regeneration period of 900 seconds) was achieved using mechanical hydrogen compression.
- The lumped thermal modeling results showed a good agreement with the measurement results.

ACKNOWLEDGEMENTS

This work was performed under Air Force SBIR Phase II Contract No. FA8650-05-C-2622. The authors wish to acknowledge the contributions of Mr. Jeff Reichl of Advanced Cooling Technologies, Inc. for his efforts in the fabrication of the metal hydride system. Also, KJK acknowledges the help from his students regarding metal hydride material fabrication.

REFERENCES

1. Chanwoo Park; Kwang J. Kim; Joseph Gottschilch and Quinn Leland, 2005, "High Performance Heat Storage and Dissipation Technology", 2005 ASME International Mechanical Engineering Congress & Exposition, Orlando, Florida, November 5-11.

2. D.L. Vrable and K.L. Yerkes, 1998, "A Thermal Management Concept for More Electric Aircraft Power System Application," SAE Transactions, 981289.
3. V. Shanmugasundaram, J.R. Brown and K.L. Yerkes, 1997, "Thermal Management of High Heat-Flux Sources Using Phase Change Materials: A Design Optimization Procedures," American Institute of Aeronautics and Astronautics, Proceedings of the 32nd Thermophysics conference, June 23-25, AIAA-97-2451.
4. Farid, Mohammed M.; Khudhair, Amar M.; Razack, Siddique Ali K.; Al-Hallaj, Said, 2004, "A review on phase change energy storage: materials and applications", Energy Conversion and Management, Vol. 45, No. 9-10, pp. 1597-1615
5. Wei, Jinjia; Kawaguchi, Yasuo1; Hirano, Satoshi1; Takeuchi, Hiromi, 2005, "Study on a PCM heat storage system for rapid heat supply", Applied Thermal Engineering, Vol. 25, No. 17-18, pp. 2903-2920
6. E.L. Huston and G.D. Sandrock, 1980, "Engineering Properties of Metal Hydrides," Journal of Less Common Metals, Vol.74, pp.435-443.
7. S. Al-Hallaj and J.R. Selman, 2000, "A Novel Thermal Management System for Electric Vehicle Batteries using Phase-Change Material," Journal of the Electrochemical Society, Vol.147, No.9, pp.3231-3236.
8. B.H. Kang, C.-W. Park, and C.S. Lee, 1996, "Dynamic Behavior of Heat and Hydrogen Transfer in a Metal Hydride Cooling System," International Journal of Hydrogen Energy, Vol.21, No.9, pp.769-774.
9. G.A. Fateev, B.H. Kang, K.J. Kim and C.-W. Park, 1996. "Numerical Simulation And Experimental Investigation of Heat Conversion Cycle in Metal Hydride Media," Heat/mass Transfer-MIF-96 Heat and Mass Transfer in Capillary-Porous Bodies, A.V. Luikov Heat and Mass Transfer Institute, Minsk, Vol.7, pp.169-182.
10. G.K. Lloyd, K.J. Kim, K.T. Feldman, Jr., and A. Razani, 1998 "Thermal Conductivity Measurements of Metal Hydride Compacts Developed for High-Power Reactors," AIAA-Journal of Thermophysics and Heat Transfer, Vol.12, No.2, pp.132-137.
11. K.J., Kim, K.T. Feldman, Jr., G.K. Lloyd and A. Razani, 1998a, "Compressor-Driven Heat Pumps Development Employing Porous Metal Hydride Compacts," ASHRAE Transactions, 1998- Winter Meeting, San Francisco, Vol.104, Pt.1, SF-98-18-4.
12. K.J. Kim, G.K. Lloyd, A. Razani, and K.T. Feldman, Jr., 1998b, "Development of LaNi₅/Cu/Sn Metal Hydride Powder Composites," Powder Technology-An International Journal, Vol.99, pp.40-45.